

DESIGN OF CASCADE CONTROLLERS FOR A HYDRAULIC ACTUATOR

Mauro A. B. Cunha¹, Raul Guenther², Edson R. De Pieri³ and Victor Juliano De Negri²

¹ Pelotas Federal Centre for Technological Education, Praça Vinte de Setembro, 455, Pelotas-RS, 96015-360, Brazil

² Federal University of Santa Catarina, Mechanical Engineering Department, Florianópolis-SC, 88040-900, Brazil

³ Federal University of Santa Catarina, Automation and System Department, Florianópolis-SC, 88040-900, Brazil
mauro@cefetrs.tche.br, guenther@emc.ufsc.br, edson@lcmi.ufsc.br, victor@emc.ufsc.br

Abstract

This paper addresses the design of the cascade controllers for the position trajectory tracking control in hydraulic actuators. The cascade strategy consists in interpreting the hydraulic actuator mathematical model as two interconnected subsystems: a mechanical subsystem driven by a hydraulic one. From this interpretation, cascade controllers with suitable properties were proposed. In this paper, in order to state the design guidelines for the cascade controllers gains, a theoretical analysis focusing on the relations between controllers gains and performance is presented. Implementation aspects required to obtain an optimised performance are also discussed. Experimental results support the design guidelines and the implementation aspects approached in this work.

Keywords: hydraulic actuators, cascade strategy, design guidelines, controller tuning, valve dynamics

This manuscript was received on 4 January 2002 and was accepted after revision for publication on 22 July 2002

1 Introduction

Hydraulic actuators can provide a power density (power/size) that cannot be matched by any other commercial technology. This fact makes these actuators to be very attractive when a high power is necessary and the available space is small. Unfortunately, these actuators present some undesirable characteristics: lightly damped dynamics, highly non-linear behaviour, and difficulties in obtaining some parameters, among others.

These undesirable characteristics complicate the controller design for high performance closed loop applications. The simple classical controllers cannot overcome the bandwidth limitation caused by the open loop poles position. The use of a linear state controller is limited due to the hydraulic actuator is highly non-linear behaviour (Virtanen, 1993).

Due to these control difficulties, a combination of control techniques offers good theoretical and experimental results. One way to combine control techniques is to use the backstepping method. Many algorithms for controlling hydraulic actuators using such a method have been proposed in the literature (Lin and Kanellakopoulos, 1997; Fialho and Balas, 1998; Yao et al, 2000).

Another way to combine different techniques is to interpret the hydraulic actuator as two interconnected subsystems: a mechanical subsystem driven by a hydraulic one (Sepelri et al, 1990; Heintze et al, 1995; Sohl and Bobrow, 1997; Guenther and De Pieri, 1997).

In Guenther and De Pieri (1997) such a method was applied to a hydraulic actuator and the resulting controller was referred to as cascade controller. The experimental and theoretical results employing this controller have demonstrated that its closed loop performance overcomes the performance obtained with classical controllers (PID and state controller), its stability is robust to parameter variation, its structure allows compensating parametric uncertainties (Guenther et al, 1998 and 2000) and the inclusion of the valve dynamics in the control algorithm (Cunha et al, 2000a).

As in others methods, an optimised performance depends on a suitable tuning of the cascade controllers gains.

This work compiles the cascade control laws and their main properties and, by a new theoretical analysis, it presents a way to optimise their performance.

The paper presents some design guidelines for the cascade controllers gains and the implementations aspects required to obtain an optimised performance.

In this paper, section 2 describes the hydraulic actuator mathematical models used in this work. In section

3, the cascade strategy is presented. Section 4 compiles the cascade controllers control laws. In section 5, the cascade structure is explored for each subsystem separately, and the relations between controller gains, parametric uncertainties and closed loop system performance are analysed. Section 6 presents the experimental implementation details. In section 7, the experimental results are presented. In section 8, the conclusions are outlined.

2 Hydraulic Actuator Mathematical Model

The hydraulic actuator considered in this work is shown in Fig. 1. It consists of a double-rod cylinder controlled by a critical centre four-way spool valve. In this modelling, it is considered that the hydraulic power unit delivers constant supply pressure p_s irrespective of the oil flow rate.

In Fig. 1, p_0 is the return pressure, p_1 is the pressure in the 1st line, p_2 is the pressure in the 2nd line, v is the total oil volume in chambers and lines, A is the cylinder piston cross-sectional area, M represents the total mass of the system, B is the viscous friction coefficient, y is the actuator piston position, F_L represents an external force, and u is the control input.

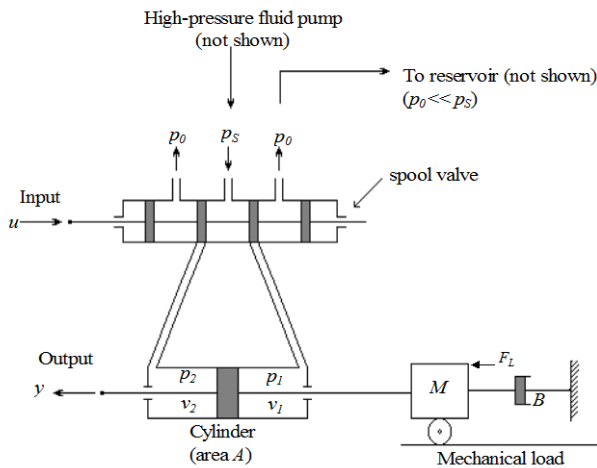


Fig. 1: Hydraulic actuator

Considering the valve dynamics as a first order system, the hydraulic actuator's non-linear mathematical model can be written as (Cunha, 2001):

$$M\ddot{y} + B\dot{y} = Ap_{\Delta} + F_L \quad (1)$$

$$\dot{p}_{\Delta} = -Af(y)\dot{y} + K_h f(y)g(x_v, p_{\Delta})x_v \quad (2)$$

$$\dot{x}_v = -\omega_v x_v + K_{em}\omega_v u \quad (3)$$

where x_v is the valve spool position, $p_{\Delta} = p_1 - p_2$ is the pressure difference in the cylinder, β is the oil bulk modulus, K_h is a hydraulic constant, K_{em} is a valve constant, and ω_v is the valve bandwidth. The non-linear function $f(y)$ and $g(x_v, p_{\Delta})$ are given by

$$f = f(y) = \frac{\beta v}{(0.5v)^2 - (Ay)^2} \quad (4)$$

$$g = g(x_v, p_{\Delta}) = \sqrt{p_s - \text{sgn}(x_v)p_{\Delta}} \quad (5)$$

Remark – The term “ x_v ” expresses the measurement in Volts of the spool displacement obtained by an internal valve transducer. In this way, K_{em} is dimensionless.

Linearising the system around origin, one obtains the hydraulic actuator linear mathematical model:

$$M\ddot{y} + B\dot{y} = Ap_{\Delta} \quad (6)$$

$$\dot{p}_{\Delta} = \frac{4\beta}{v}(K_Q x_v - K_C p_{\Delta} - Ay) \quad (7)$$

$$\dot{x}_v = -\omega_v x_v + K_{em}\omega_v u \quad (8)$$

where K_Q is the flow rate gain and K_C is the flow rate pressure gain.

When the valve dynamics is sufficiently fast and can be neglected, the non-linear system represented by Eq. 1, 2 and 3 are reduced to a third order non-linear model:

$$M\ddot{y} + B\dot{y} = Ap_{\Delta} + F_L \quad (9)$$

$$\dot{p}_{\Delta} = -Af(y)\dot{y} + K_{hu}f(y)g_u(u, p_{\Delta})u \quad (10)$$

where $K_{hu} = K_{em}K_h$ and the non-linear function $g_u(u, p_{\Delta})$ is given by

$$g_u = g_u(u, p_{\Delta}) = \sqrt{p_s - \text{sgn}(u)p_{\Delta}} \quad (11)$$

Linearising Eq. 10, one obtains the third order hydraulic actuator linear model:

$$M\ddot{y} + B\dot{y} = Ap_{\Delta} \quad (12)$$

$$\dot{p}_{\Delta} = \frac{4\beta}{v}(K_{Qu}u - K_C p_{\Delta} - Ay) \quad (13)$$

where $K_{Qu} = K_{em}K_Q$ is the new flow rate gain.

The four models presented in this section will be used in the sequel.

3 The Cascade Strategy

The hydraulic actuator can be interpreted as two interconnected subsystems: a mechanical subsystem driven by a hydraulic one. This interpretation is shown in Fig. 2 and can be explained physically.

In the hydraulic actuator shown in Fig. 1, when the valve spool is moved in one direction, the pressure in one chamber starts to increase and the pressure in the other chamber starts to decrease. It creates a pressure difference p_{Δ} between the chambers and generates a force on the piston actuator. This force is applied to a mass-damper system (mechanical subsystem). Therefore, the mechanical subsystem is driven by a hydraulic one. On the other hand, the piston movement affects the fluid pressure in the chambers of the hydraulic subsystem, and this shows the system interconnection.

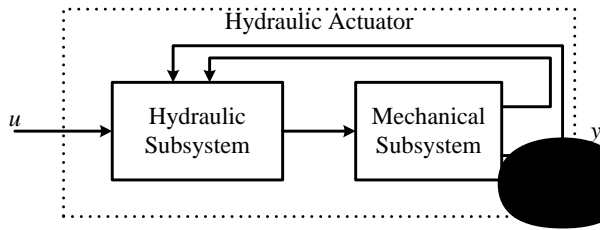


Fig. 2: Interconnected subsystems

This interpretation is used by several authors to develop controllers for hydraulic actuators (Sepehri et al, 1990; Heintze et al, 1995; Sohl and Bobrow, 1997). The idea is to promote a fast loop in the hydraulic subsystem in order to generate a force in the hydraulic subsystem that allows the mechanical subsystem to track the desired trajectory.

In Guenther and De Pieri (1997) this idea was formalised taking into account an error during the hydraulic subsystem trajectory tracking and by presenting a stability proof of the whole interconnected system. The resulting strategy is presented in the sequel.

The control objective is that $y(t)$ tracks a desired trajectory $y_d(t)$ as closed as possible. To achieve this end, let

$$\tilde{p}_\Delta = p_\Delta - p_{\Delta d} \quad (14)$$

be the pressure difference tracking error, where $p_{\Delta d}$ is the desired pressure difference so that the control goal is reached. Substituting Eq. 14 into Eq. 1 gives

$$M\ddot{y} + B\dot{y} = A p_{\Delta d} + d(t) \quad (15)$$

where $d(t) = A\tilde{p}_\Delta + F_L$ is an input disturbance.

The system in Eq. 15, 2 and 3 is in the cascade form. Equation 15 can be interpreted as a second order mechanical subsystem driven by a desired force $A p_{\Delta d}$ and subjected to an input disturbance $d(t)$. Equation 2 and 3 represent the hydraulic subsystem.

The design of the cascade controller for the system in Eq. 15, 2 and 3 can be summarised as:

- Compute a control law $p_{\Delta d}$ to the mechanical subsystem in Eq. 15 such that the cylinder displacement achieves a desired trajectory $y_d(t)$ taking into account the presence of the disturbance $d(t)$. With this desired force $A p_{\Delta d}$ one can quantify the desired pressure difference;
- Compute a control law u such that p_Δ tracks $p_{\Delta d}$ defined above as closed as possible.

4 The Cascade Controllers

According to the strategy described above and considering the linear model in Eq. 12 and 13, Guenther and De Pieri (1997) proposed a cascade controller that combines a control law for the mechanical subsystem based on a fixed Slotine and Li's scheme (Slotine and Li, 1988) with a control law for the hydraulic subsystem that is basically a computed force scheme (similar to the computed torque used in robotics) with a proportional term.

The exponential stability of the whole system was demonstrated by using the Lyapunov's direct method, in the case that all the system parameters are exactly known. When there are uncertainties in the system parameters, the tracking errors go to a bounded region that can be decreased by increasing the controller gains (Cunha et al, 1997).

From these results, the algorithm has evolved in order to consider the non-linear model, the parametric uncertainties, and the valve dynamics. The corresponding control laws are compiled in this section (see also Cunha et al, 2000b).

4.1 Fixed Cascade Controller (CC)

In this case, the desired pressure difference required to track y_d as closed as possible is calculated by using a Slotine and Li (1988) control law given by

$$p_{\Delta d} = \frac{1}{A} (M\dot{y}_r + B\dot{y}_r - K_D z) \quad (16)$$

$$\dot{y}_r = \dot{y}_d - \lambda \tilde{y}, \quad \tilde{y} = y - y_d, \quad z = \dot{y} - \dot{y}_r = \dot{y} + \lambda \tilde{y} \quad (17)$$

where \tilde{y} is the position trajectory tracking error, \dot{y}_r is a reference velocity, z is a measure of the trajectory tracking error, and $K_D > 0$ and $\lambda > 0$ are the mechanical subsystem control law gains.

The hydraulic subsystem control law contains the inverse of the functions $f(y)$ and g_u , defined in Eq. 4 and 11 respectively, and is given by

$$u = \frac{1}{K_{hu} g_u} \left[\frac{1}{f(y)} (\dot{p}_{\Delta d} - K_{P1} \tilde{p}_\Delta) + A\dot{y} \right] \quad (18)$$

where K_{P1} is the proportional gain, and $\dot{p}_{\Delta d}$ is the time derivative of the desired pressure difference given in Eq. 16.

The computation of $\dot{p}_{\Delta d}$ involves the relationships $y_r^{(3)}$ and \dot{z} . From Eq. 17, one concludes the necessity of the knowledge of the cylinder acceleration \ddot{y} . In the case that all parameters related to the mechanical subsystem are known and there is no external force ($F_L = 0$), \ddot{y} can be computed by using Eq. 9.

It should be remarked that if the mechanical subsystem parameters have uncertainties and/or there is an external force, using Eq. 9 and the mechanical subsystem nominal parameters, one obtains only a nominal value for the time derivative of the desired pressure difference ($\dot{p}_{\Delta d0}$). The error in this time derivative ($\dot{\tilde{p}}_{\Delta d} = \dot{p}_{\Delta d} - \dot{p}_{\Delta d0}$) originates a tracking error in the hydraulic subsystem that may be minimised by using a variable structure term, as it is explained in the next subsection.

The cascade controller is obtained by combining Eq. 16 and 18, and it needs only the state variables, namely the position y , the velocity \dot{y} and the pressure difference p_Δ , to be implemented. A block diagram displaying the CC control structure is shown in Fig. 3.

The complete controller design comprises the tuning of the gains K_D , λ , and K_{P1} , and will be discussed in section 5.

Eq. 1, as it was discussed in subsection 4.2. In this way, the implementation of this controller needs only the state variables, namely the position y , the velocity \dot{y} , the pressure difference p_Δ and the spool position x_v .

This controller design comprises the tuning of the gains K_D , λ , K_{P1} , K_{P2} and K_V , and it is presented in the following guidelines.

5 Design Guidelines

In order to obtain a good closed loop performance, it is necessary to optimise the tuning of the controller gains. To achieve this goal, it is necessary to know how each gain influences the system response. Aiming to give this answer, this section presents some design guidelines for the cascade controllers presented in section 4. These guidelines are obtained by analysing the closed loop performance with relation to the gains and parametric uncertainties.

5.1 Mechanical Subsystem Gains (K_D and λ)

In this subsection, a way is proposed to tune the gains K_D and λ . The gain maximised, in order to reduce the influence of the parametric uncertainties. This gain is limited by the sample rate and the sensors noise. In sequence, the value of λ is increased up to the point that vibrations occur.

To show that \dot{y}_r , \ddot{y}_r and z (Eq. 17) are rewritten as a function of y and y_d :

$$\dot{y}_r = \dot{y}_d + \lambda y_d - \lambda y \quad (24)$$

$$\ddot{y}_r = \ddot{y}_d + \lambda \dot{y}_d - \lambda \dot{y} \quad (25)$$

$$z = -\dot{y}_d - \lambda y_d + \dot{y} + \lambda y \quad (26)$$

Substituting Eq. 24, 25 and 26 into the mechanical subsystem control law, Eq. 16, gives

$$p_{\Delta d} = \frac{1}{A_0} \left[M_0 \ddot{y}_d + (\lambda M_0 + B_0 + K_D) \dot{y}_d + \lambda (B_0 + K_D) y_d - (\lambda M_0 + K_D) \dot{y} - \lambda (B_0 + K_D) y \right] \quad (27)$$

where $(\cdot)_0$ are the nominal parameters used in the control law design.

Considering that the hydraulic actuator area can be measured with the required precision (i.e., $A = A_0$) and substituting Eq. 27 into Eq. 1 (mechanical subsystem), one obtains

$$\begin{aligned} M\ddot{y} + (\lambda M_0 + B + K_D)\dot{y} + \lambda(B_0 + K_D)y &= \\ = M_0\ddot{y}_d + (\lambda M_0 + B_0 + K_D)\dot{y}_d + \lambda(B_0 + K_D)y_d & \quad (28) \\ + A\tilde{p}_\Delta + F_L \end{aligned}$$

Applying the Laplace transform with null initial conditions to Eq. 28 gives

$$Y(s) = C_1(s)Y_d(s) + C_2(s)(A\tilde{P}_\Delta(s) + F_L(s)) \quad (29)$$

where s is the Laplace variable and

$$C_1(s) = \frac{M_0 s^2 + (\lambda M_0 + B_0 + K_D)s + \lambda(B_0 + K_D)}{M s^2 + (\lambda M_0 + B + K_D)s + \lambda(B_0 + K_D)} \quad (30)$$

$$C_2(s) = \frac{1}{M s^2 + (\lambda M_0 + B + K_D)s + \lambda(B_0 + K_D)} \quad (31)$$

Analysing Eq. 31, one concludes that the $C_2(s)$ transfer function DC gain is equal to $1/(\lambda(B_0 + K_D))$. It means that the higher K_D and λ are, the smaller are the external disturbance and pressure difference tracking error influences upon the position tracking.

Now, considering that $M = M_0$, and that K_D may be designed such that $K_D \gg B$ and $K_D \gg B_0$, the $C_1(s)$ and $C_2(s)$ transfer function can be written as

$$C_1(s) \cong 1 \quad (32)$$

$$C_2(s) \cong \frac{1}{M} \frac{1}{(s + \lambda) \left(s + \frac{K_D}{M} \right)} \quad (33)$$

In this case, by designing λ such that $K_D / M \gg \lambda$, one can analyse $C_2(s)$ as

$$C_2(s) \cong \frac{1}{\lambda K_D} \frac{\lambda}{(s + \lambda)} \quad (34)$$

From Eq. 29 with $C_1(s)$ and $C_2(s)$ represented by Eq. 32 and 34, respectively, gives

$$\tilde{Y}(s) \cong C_2(s)(F_L(s) + A\tilde{P}_\Delta(s)) \quad (35)$$

where $\tilde{Y}(s) = Y(s) - Y_d(s)$.

From this equation one concludes that increasing the gain λ , the $C_2(s)$ transfer function DC gain is decreased and the bandwidth of $C_2(s)$ is increased. Then, if on the one side the influence of \tilde{p}_Δ and F_L in the trajectory tracking error \tilde{y} is decreased by increasing λ , on the other side the high frequency components existing in those signals can cause vibrations in the actuator due to the extended bandwidth.

Therefore, the controller gain tuning is done by choosing K_D as great as possible (limited by the vibrations caused by the sample rate and the sensors noise) and, in the sequence, increasing the value of λ up to the point that the actuator starts to vibrate.

5.2 Hydraulic Subsystem Gains

[1] The Proportional Gain K_{P1} in CC and VS-ACC

The CC and VS-ACC theoretical synthesis and analysis are based on a hydraulic actuator mathematical model that does not take into account the valve dynamics. In this way, theoretically, the gain K_{P1} in Eq. 18 and 21 could be unbounded. In experimental implementation, however, it is observed that this gain causes oscillations in the piston position if it is greater than some value. In this subsection the relationship between this limit in the proportional gain and the valve dynamics is discussed.

To establish the design rules for the hydraulic subsystem proportional gain, consider the valve dynamics as a first order system and the linearised hydraulic subsystem given by Eq. 7 and 8. The linearised version for the hydraulic subsystem control law in Eq. 18 is given by

$$u = \frac{1}{K_{Qu}} \left[A\dot{y} + \frac{v}{4\beta} (\dot{P}_{\Delta d} - K_{P1} \tilde{P}_{\Delta}) \right] \quad (36)$$

As the flow rate pressure gain K_C is small in this analysis one considers $K_C = 0$. Combining Eq. 7 and 8, substituting Eq. 36 into this combination, and applying the Laplace transform with null initial conditions gives

$$P_{\Delta}(s) = \frac{4\beta}{v} \left(-AY + \frac{\omega_v}{s + \omega_v} AY \right) + \frac{1}{s} \left\{ \frac{\omega_v}{s + \omega_v} [sP_{\Delta d} - K_{P1} (P_{\Delta} - P_{\Delta d})] \right\} \quad (37)$$

Equation 37 can be written as

$$P_{\Delta}(s) = \frac{\omega_v (s + K_{P1})}{s^2 + \omega_v s + K_{P1} \omega_v} P_{\Delta d}(s) - P_{\text{dist}}(s) \quad (38a)$$

where

$$P_{\text{dist}}(s) = \frac{4\beta A}{v} \frac{1}{s^2 + \omega_v s + K_{P1} \omega_v} \ddot{Y} \quad (38b)$$

represents a disturbance in the hydraulic subsystem tracking and $\ddot{Y}(s) \equiv s^2 Y(s)$.

In the case that $P_{\text{dist}}(s)$ is neglected, one obtains

$$P_{\Delta}(s) = \frac{\omega_v (s + K_{P1})}{s^2 + \omega_v s + K_{P1} \omega_v} P_{\Delta d}(s) \quad (39)$$

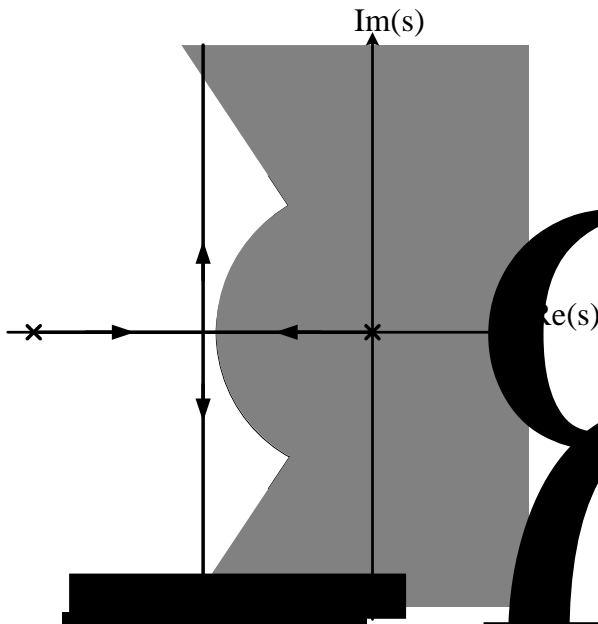


Fig. 4: Root locus of $\frac{P_{\Delta}(s)}{P_{\Delta d}(s)}$ in function of K_{P1}

From Eq. 39, one concludes that if the valve dynamics is represented by a first order system, the relation between $P_{\Delta d}(s)$ and $P_{\Delta}(s)$ is a second order system in which the poles position and, consequently, the behaviour depends on the valve bandwidth and the gain K_{P1} . When the gain K_{P1} is small (near zero), the transfer function presents two poles on the left real axis, one near the origin (dominant) and the other more to the

left. As the gain K_{P1} is increased, the system becomes critically damped and, in the sequence, underdamped. Figure 4 illustrates this situation, where the region on left of the dark region represents the allowable part where the poles must be located to obey the design requirements.

From Eq. 39, one verifies that the faster the valve dynamics is, the larger is the value of the gain K_{P1} that can be used without the system to be underdamped. The hydraulic subsystem underdamped behaviour, depending on the desired pressure trajectory characteristics, may cause oscillations in the pressure difference p_{Δ} and, consequently, in the piston position y . This explains the oscillations observed in the experiments.

When this analysis is performed considering the valve dynamics as a second order system, the relation between $P_{\Delta d}(s)$ and $P_{\Delta}(s)$ is a third order system that may be unstable depending on the valve bandwidth and the gain K_{P1} .

The system performance requirements (dark region in Fig. 3) and Eq. 39 allow designing the proportional gain of the hydraulic subsystem.

[2] The Gains K_{P1} , K_{P2} and K_V in NFCC

In the NFCC controller the gain K_{P1} could be theoretically unbounded. In practice, it is limited by the sample rate and by the sensors noise.

The gain K_V is tuned in order to obtain a specified performance and the gain K_{P2} is tuned starting from a small value up to a limit in which the actuator presents oscillations. This rules come from the valve closed loop analysis presented in this subsection.

Substituting the control law, Eq. 23, into Eq. 3, one obtains the valve closed loop equation:

$$\dot{x}_v = -\omega_v x_v + \Delta K \frac{\omega_v}{\omega_{v0}} (\dot{x}_{vd} + \omega_{v0} x_v - f_0 K_{h0} g K_{P2} \tilde{p}_{\Delta} - K_V \tilde{x}_v) \quad (40)$$

where $\Delta K = K_{em} / K_{em0}$.

To satisfy the stability requirements when the nominal system parameters are known, only $K_{P2} > 0$ must hold. Consider firstly that the gain K_{P2} is sufficiently small such that the term $f_0 K_{h0} g K_{P2} \tilde{p}_{\Delta}$ can be neglected. In this case, applying the Laplace transform to Eq. 40, one obtains

$$X_v(s) = \frac{\Delta K \frac{\omega_v}{\omega_{v0}} (s + K_V)}{s + \omega_v (1 - \Delta K) + \Delta K \frac{\omega_v}{\omega_{v0}} K_V} X_{vd}(s) \quad (41)$$

In order to stabilize this transfer function, the K_V gain must be designed such that

$$K_V > \frac{\omega_{v0} (\Delta K - 1)}{\Delta K} \quad (42)$$

The inequality in Eq. 42 is easily satisfied, since that K_{em} can be determined with a required precision, i.e., $\Delta K \cong 1$. Using that consideration, one has

$$X_v(s) = T_1(s) X_{vd}(s) \quad (43)$$

where

$$T_1(s) = \frac{\frac{\omega_v}{\omega_{v0}}(s + K_V)}{s + \frac{\omega_v}{\omega_{v0}}K_V} \quad (44)$$

From this transfer function, one concludes that the pole location of $T_1(s)$ is given by $(\omega_v / \omega_{v0}) K_V$, i.e., the gain K_V can be adjusted to state the desired performance.

Additionally, one can also conclude that the DC gain of $T_1(s)$ is unitary independent of the parametric uncertainty upon ω_v and the parametric uncertainty upon valve dynamics does not allow the pole-zero cancellation.

The system behaviour with relation to K_{p2} was experimentally observed and it is shown to depend on the K_V , ω_{v0} and K_{em0} values. The value of this gain is adjusted starting from a small value until vibrations of the piston actuator occur.

5.3 The Adaptation Gains and the Modulation Function

The adaptation gains in the diagonal matrix Γ and the modification term σ_s are tuned in order to obtain a smooth estimated parameter response and to guarantee the estimated parameter boundness. Usually simulations may help to achieve this goal.

The modulation function $m(t)$ in the control law in Eq. 21 is designed such that

$$m(t) \geq \left| \dot{\tilde{p}}_{Ad}(t) \right| \quad (45)$$

where $\dot{\tilde{p}}_{Ad} = \dot{p}_{Ad} - \dot{p}_{Ad0}$ is the error in the time derivative \dot{p}_{Ad} .

5.4 Smoothing the Signum Function $\text{sgn}(\tilde{p}_\Delta)$

The use of the non-linear function $\text{sgn}(\tilde{p}_\Delta)$ in the control law in Eq. 21 may cause chattering in the actuator piston position y . In order to avoid this problem, the signum function $\text{sgn}(\tilde{p}_\Delta)$ may be substituted by a saturation function $\text{sat}(\tilde{p}_\Delta/\varepsilon)$ defined by

$$\text{sat}\left(\frac{\tilde{p}_\Delta}{\varepsilon}\right) = \begin{cases} \frac{\tilde{p}_\Delta}{\varepsilon}, & \text{if } \left| \frac{\tilde{p}_\Delta}{\varepsilon} \right| \leq 1 \\ \text{sgn}\left(\frac{\tilde{p}_\Delta}{\varepsilon}\right), & \text{if } \left| \frac{\tilde{p}_\Delta}{\varepsilon} \right| > 1 \end{cases} \quad (46)$$

where $\varepsilon > 0$ is the boundary layer width (Slotine and Li, 1991).

6 Experimental Implementation

Besides the design guidelines described in section 5, the results of an experimental implementation depend on the choice of a suitable sample period and on the conditioning of the measured signals with respect to the noise.

Furthermore, as a proportional valve with overlap is

used in the hydraulic actuator shown in Fig. 1. There is a dead-zone in the relation between the signal input and the flow rate. In this way, the implementation also depends on a suitable dead-zone compensation.

In this section, after describing the experimental setup, we discuss these implementation details.

6.1 Experimental Setup

The experimental implementation was performed on a test rig composed of a double-rod cylinder, a proportional valve NG6 – BOSH and its electronic card, a data acquisition and control board DS 1102 dSPACE, pressure transducers, temperature transducers installed between the valve and actuator, position transducer, and a conditioning and power hydraulic unit. The conditioning and power hydraulic unit and the hardware for control scheme are shown in Fig. 5 and 6, respectively.



Fig. 5: Experimental setup - Laboratory of Hydraulic and Pneumatic Systems (LASHIP) at Federal University of Santa Catarina

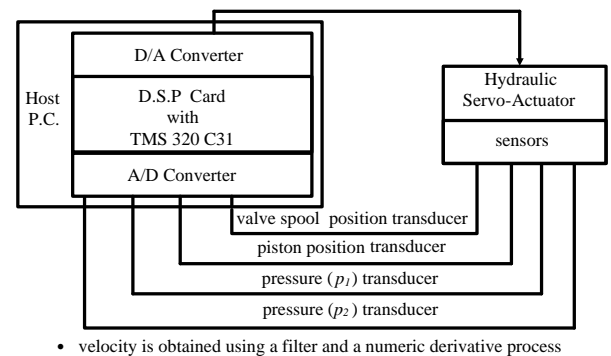


Fig. 6: Hardware for control scheme

Considering the models presented in section 2, the system parameters are $M = 20.66 \text{ kg}$, $B = 316 \text{ Nsm}^{-1}$, $A = 7.6576 \times 10^{-4} \text{ m}^2$, $\beta = 10 \times 10^8 \text{ Nm}^2$, $v = 9.5583 \times 10^{-4} \text{ m}^3$ and $p_s = 10 \text{ MPa}$. The cylinder stroke is 1 meter ($|y_{\max}| = 0.5 \text{ m}$). The valve manufacturer declares the nominal flow rate to be 35 l/min at a pressure differential of 0.8 MPa. In this practical application the input u is the electronic amplifier input and u can assume values between -10 V and +10 V, $K_{em} = 0.76$, $K_h = 6.55 \times 10^{-8} \text{ m}^4 \text{V}^{-1} \text{s}^{-1} \text{N}^{-1/2}$.

The NG6 valve with WV 45 – RGC electronic card presents the following characteristics: 0.3 % of hysteresis, 0.2 of range of inversion, 30×10^{-3} s of response time for 100 % signal change and 15×10^{-3} s of response time for 10 % signal change.

6.2 Sample Period

When a continuous controller is implemented by using a microprocessor-based system, the sample rate limits the closed loop bandwidth and, consequently, the system closed loop performance.

According to the design rules stated in this work, the subsystem closed loop dominant pole is given by λ . In this way, the sample frequency in [rad/s] must be at least 20 times the greatest value of λ .

Among others, the sample period depends on the system processor clock and on the number of machine cycles required to perform the whole control algorithm at each step.

In this implementation, the controller board has a signal processor of 40 MHz. By using this apparatus, the minimum sample period possible with these cascade controllers was 5×10^{-3} s, i.e., the sample frequency is 1256 rad/s.

6.3 Filters

The filters were used to decrease the noise in the measured signals by the sensors, which limit the control gains and, consequently, the closed loop performance. On the other side, the filters cause a delay in each measured signal and, in consequence, they may limit the closed loop performance too. In this way, there is a trade-off between the noise reduction and the delay.

The signal of each transducer was filtered through a first order system and adjusted by the transducers inverse calibration curves. The filters have bandwidth $\omega_{iy} = 80$ rad/s (position), $\omega_{ip} = 100$ rad/s (pressure) and $\omega_{ixv} = 100$ rad/s (spool valve).

Analysing the used sample period, one can see that the filters could be adjusted with greater values. However, due to the significant sensors noise, they had to be adjusted with small values. Consequently, it decreases the closed loop performance.

6.4 Dead-Zone Compensation

Usually, the valve is commanded by an electronic card with a circuit that reproduces a dead-zone inverse, which may be used to compensate the valve dead-zone. This electronic card also has an electrical dead-zone in its input (Virvalo, 1997). Therefore, even if the valve dead-zone could be compensated by the electronic card circuit, there would be a dead-zone in the relation between the electronic card input voltage and the flow rate in the valve, caused by this electrical dead-zone. To overcome this problem, one proposes a dead-zone compensation placed between the control signal u generated by the control algorithm and the D/A converter (voltage applied to the electronic card).

In this case, the used dead-zone compensation is given by

$$u_{ec} = \begin{cases} u + l_c & \text{para } u < -s_b \\ \frac{-l_c}{s_b} u & \text{para } -s_b \leq u < 0 \\ \frac{r_c}{s_b} u & \text{para } 0 \leq u \leq s_b \\ u + r_c & \text{para } u > s_b \end{cases} \quad (47)$$

where s_b and r_c are positive constants and l_c is a negative constant. Figure 7 illustrates this compensation.

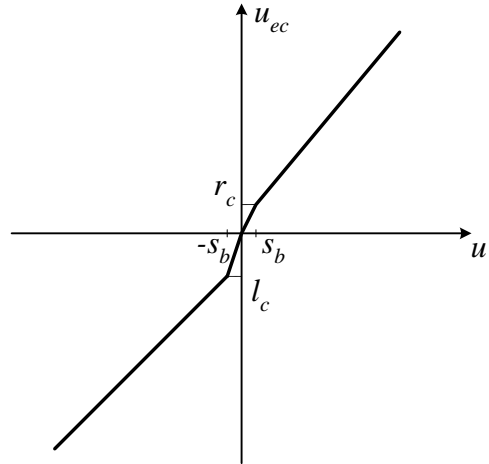


Fig. 7: Dead-zone compensation

6.5 Spool Position Measurement Scheme

The valve spool position is one of the signals used in the NFCC control law (Eq. 23). The NFCC was designed for a critical centre valve, in which there is no dead-zone. Note that the proposed dead-zone compensation (subsection 6.4) causes a fixed shift of the valve spool when a voltage is applied. Therefore, this shift caused by the compensation must be eliminated to obtain the spool position. To achieve this goal, one proposes the inclusion of a dead-zone to measure the spool position as shown in Fig. 8, where $e_{rc} > 0$ and $e_{lc} < 0$ are the values that limit the dead-zone region (Cunha et al, 2000a).

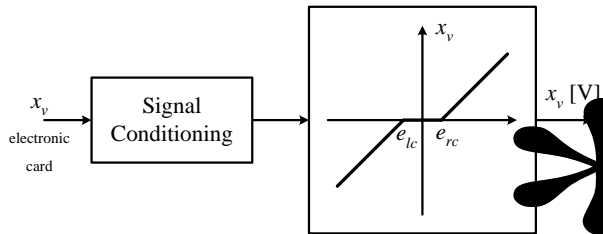


Fig. 8: Scheme for measuring the spool position

7 Experimental Results

This section presents the experimental results obtained with the cascade controllers designed according to the guidelines described in section 5. Here, the importance of the sample period, of the dead-zone compensation, of the parametric uncertainties and of considering the valve dynamics is outlined.

A PΔP controller, which combines a P controller with a pressure feedback, is also testified for comparison.

7.1 CC Controller

The controller gains K_D , λ and K_{P1} are firstly obtained by following the design guidelines described in section 5. The final tuning is done by increasing the values of these gains up to the point in which the control signal presents oscillations. The first gain to be adjusted is K_{P1} . It is done by analysing the pressure difference error \bar{p}_Δ obtained experimentally. In the sequence, the value of K_D is increased to the maximum value in order to minimise the uncertainties effects, by analysing the trajectory tracking error. To finish, the λ value is tuned in the same way.

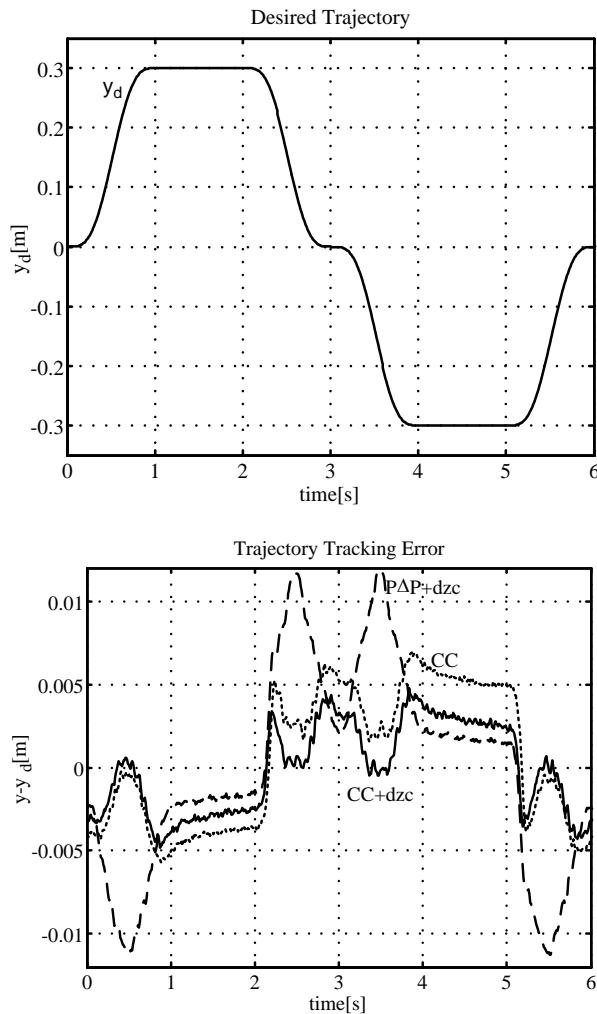


Fig. 9: Responses to CC without dead-zone compensation, to CC with dead-zone compensation (CC+dzc) and to PΔP with dead-zone compensation (PΔP+dzc)

Figure 9 shows the results obtained with the CC controller with and without dead-zone compensation and with the PΔP controller with dead-zone compensation. These controllers were testified in the closed loop with a sample period of 1×10^{-3} s and the following gains: $K_D = 11000 \text{ Nsm}^{-1}$, $\lambda = 25 \text{ s}^{-1}$ and $K_{P1} = 500 \text{ s}^{-1}$. The PΔP controller was tuned with a proportional gain of 400 Vm^{-1} and a feedback pressure gain of $2 \times 10^{-9} \text{ VPa}^{-1}$. The dead-zone compensation (dzc) parameters were adjusted as $l_c = -0.7 \text{ V}$, $r_c = 0.3 \text{ V}$ and $s_b = 0.05 \text{ V}$.

Analysing Fig. 9, one can see that the cascade controller presents smaller trajectory tracking errors and greater final position errors when compared to the PΔP controller. One can also observe that there is a considerable static error caused by the valve dead-zone and the dry-friction. This error is decreased by using the compensation presented in subsection 6.4. Note that the different values of r_c and l_c compensate the valve asymmetric dead-zone.

Decreasing the sample period, is a proper mean to increase the controller gains without causing actuator vibration. In this case, decreasing the sample period from 1×10^{-3} s to 5×10^{-3} s, the value of λ was increased from 25 s^{-1} to 35 s^{-1} . A comparison between these two results is shown in Fig. 10.

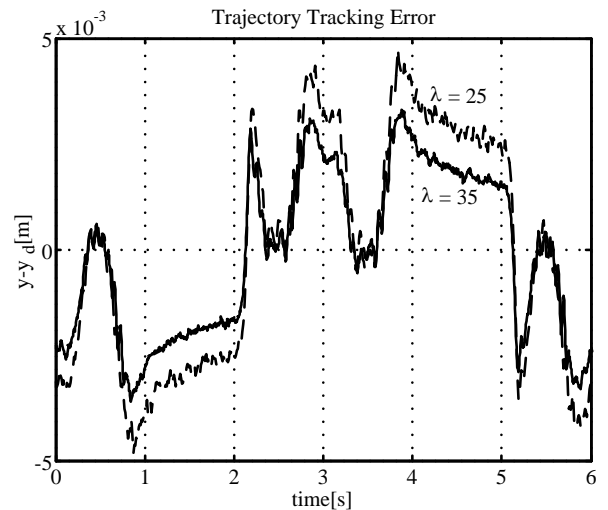


Fig. 10: Responses to CC with $\lambda = 25 \text{ s}^{-1}$ and $\lambda = 35 \text{ s}^{-1}$ with dead-zone compensation

7.2 VS-ACC Controller

The controller gains (K_{P1} , K_D and λ) are tuned in the same way as the CC controller.

The modulation function is calculated from inequality in Eq. 45 or may be adjusted experimentally as a fixed value $\bar{m} \geq |\dot{\bar{p}}_\Delta(t)|$, in order to obtain stability. The switching region is adjusted experimentally. These controller parameters were adjusted as $m = 2 \times 10^8 \text{ Pa}$, $\Gamma = \text{diag}(10^3, 10^3)$, $\sigma_s = 2$.

In order to show the effect of adaptation in the VS-ACC controller, a value of mass of 10 times the real nominal value is set as the nominal value in the CC and VS-ACC controllers. Analysing the experimental results shown in Fig. 11, one verifies that, in this case, the

VS-ACC improves the system performance.

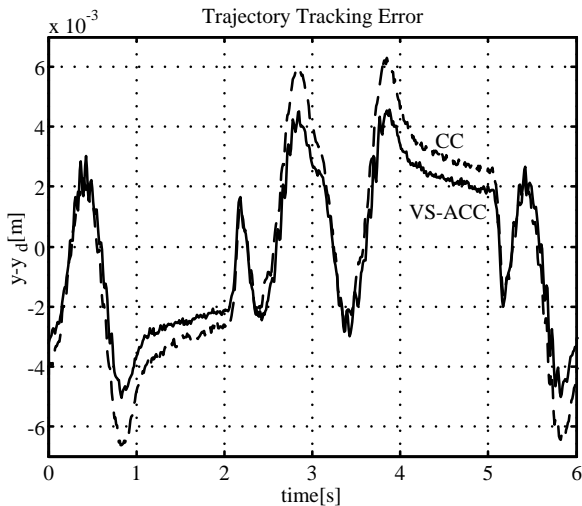


Fig. 11: Responses to CC and VS-ACC with mass uncertainty and dead-zone compensation

7.3 NFCC Controller

Besides the gains K_D , λ and K_{P1} , the NFCC implementation comprises the tuning of the gains K_V and K_{P2} . As described in section 5, the gain K_{P2} is adjusted from a small value that is increased up to the point in which the piston actuator presents oscillations. The gain K_V is firstly obtained by Eq. 44, and in the sequence being tuned experimentally.

An experimental result comparing this controller to the CC with nominal parameters is shown in Fig. 12. In this case, the cascade controllers were tuned with $K_D = 11000 \text{ Nsm}^{-1}$, $\lambda = 30 \text{ s}^{-1}$, $K_{P1} = 500 \text{ s}^{-1}$, $K_{P2} = 1 \times 10^{-15} \text{ m}^2 \text{Pa}^{-2}$ and $K_V = 350 \text{ s}^{-1}$. The dead-zone compensation parameters were set to $l_c = -0.7 \text{ V}$, $r_c = 0.3 \text{ V}$ and $s_b = 0.05 \text{ V}$.

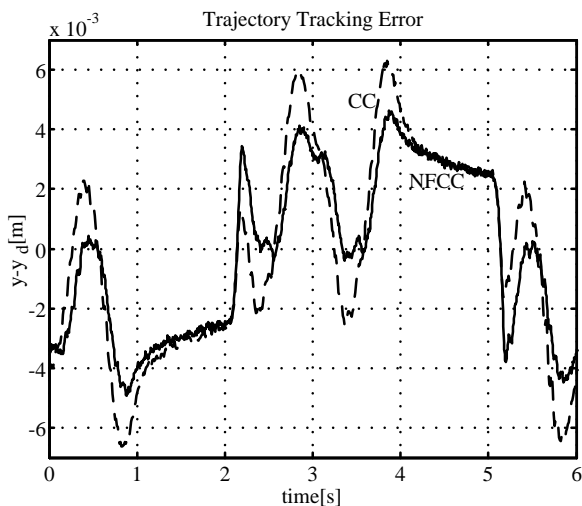


Fig. 12: Responses to CC and NFCC with dead-zone compensation

In this comparison, the NFCC presented a better performance. It is important to outline that in this case the valve dynamics is of substantial importance mainly

because the load is small ($M = 20.66 \text{ kg}$).

These experimental results demonstrate that a suitable compensation of the dead-zone can improve substantially the closed loop performance. Additionally, the inclusion of the valve dynamics when the valve bandwidth is limited has shown to be very important. It was also demonstrated that decreasing the sample period, helps to increase the controller gains and, consequently, to decrease the trajectory tracking errors.

8 Conclusions

In this work, the cascade control laws for a hydraulic actuator and their main properties were compiled, and a new theoretical analysis of the closed loop system was presented.

This analysis allows one to state the influence of the controller gains in the closed loop performance and, consequently, to state some design guidelines for the controller gains aiming to obtain an optimised performance. In this new analysis, some performance limitations and a way to overcome them were also discussed. Additionally, experimental aspects required for an optimised implementation were also approached.

The results presented in this paper provide the design guidelines of the cascade controllers for many practical applications, and they have currently been applied to the research of cascade controllers for hydraulic actuators with friction compensation and for hydraulic manipulators.

Nomenclature

A	Cylinder piston area
B	Viscous friction coefficient
f	Non-linear function
g	Non-linear function
K_D	Controller gain
K_{em}	Valve constant
K_h	Hydraulic constant
K_{hu}	Hydraulic constant
K_{P1}	Controller gain
K_{P2}	Controller gain
K_V	Controller gain
m	Modulation function
M	System's total mass
p_1	Pressure in the 1 st line
p_2	Pressure in the 2 nd line
p_Δ	Pressure difference
$p_{\Delta d}$	Desired pressure difference
\tilde{p}_Δ	Pressure difference tracking error
s	Laplace variable
u	Control law
v	Total volume
V	Lyapunov function
x_v	Spool position
x_{vd}	Desired spool position
\tilde{x}_v	Valve spool position error
y_d	Desired trajectory

y_r	Reference velocity
\tilde{y}	Position trajectory tracking error
z	Measure of the trajectory tracking error
β	Oil bulk modulus
Γ	Adaptation gains matrix
λ	Controller gain
σ_s	Modification term
$\hat{\theta}$	Estimated parameter vector

References

- Cunha, M. A. B., Guenther, R. and De Pieri, E. R.** 1997. Robustness Analysis of Cascade Controller Applied to a Hydraulic Actuator. *Proceedings of XII Congreso Chileno de Ingeniería Eléctrica*, Temuco, Vol. 2, pp. 479-484.
- Cunha, M. A. B., Guenther, R., De Pieri, E. R. and De Negri, V. J.** 2000a. A Fixed Cascade Controller Applied to a Hydraulic Actuator Including the Servo-valve Dynamic. *Power Transmission and Motion Control 2000*, Ed. C. R. Burrows; K. A. Edge (University of Bath), Suffolk: Professional Engineering Publishing, 2000, pp. 59-72.
- Cunha, M. A. B., Guenther, R., De Pieri, E. R. and De Negri, V. J.** 2000b. A Cascade Strategy Using Nonlinear Control Techniques Applied to a Hydraulic Actuator. *Proceedings of the 1st Fluid Power Net International – PhD Symposium*, Hamburg 2000, pp. 57-70.
- Cunha, M. A. B.** 2001. Cascade Control of a Hydraulic Actuator: Theoretical and Experimental Contributions (In Portuguese). *PhD Thesis, Electrical Engineering Department*, Federal University of Santa Catarina, Brazil.
- Fialho, I. and Balas, G.** 1998. Adaptive Vehicle Suspension Design Using LPV Methods. *Proceedings of 37 IEEE Conference on Decision & Control*, Tampa, pp. 469-474.
- Guenther, R. and De Pieri, E. R.** 1997. Cascade Control of the Hydraulic Actuators. *Journal of the Brazilian Society Mechanical Sciences*, V. 19, No. 2 (Jun.), pp. 108-120.
- Guenther, R.; Cunha, M. A. B. and De Pieri, E. R.** 1998. Experimental Implementation of the Variable Structure Adaptive Cascade Control for Hydraulic Actuators. In: *Power Transmission and Motion Control*, Ed. C. R. Burrows; K. A. Edge (University of Bath), Suffolk: Professional Engineering Publishing, 1998. pp. 349-361.
- Guenther, R., Cunha, M. A. B., De Pieri, E. R. and De Negri, V. J.** 2000. VS-ACC Applied to a Hydraulic Actuator. *Proceedings of American Control Conference*, Chicago, pp. 4124-4128.
- Heintze, J., Peters, R. M. and Weiden.** 1995. Cascade Δp and sliding mode for hydraulic actuators. *Proceedings of the 3rd European Control Conference*, Roma, Italy, pp. 1471-1477.
- Lin, J. - S. and Kanellakopoulos, I.** 1997. Modular Adaptive Design for Active Suspensions. *Proceedings of the 36th IEEE Conference on Decision & Control*, California, pp. 3626-3631.
- Sepehri, N., Dumont, G. A. M., Lawrence, P. D. and Sassani, F.** 1990. Cascade Control of Hydraulically Actuated Manipulators. *Robotica*, Vol. 8 (Jul./Sep.), pp. 207-216.
- Slotine, J. - J. and Li, W.** 1988. Adaptive Manipulator Control: A Case Study. *IEEE Transaction on Automatic Control*, pp. 33-11.
- Slotine, J. - J. and Li, W.** 1990. *Applied Nonlinear Control*, 1st ed. USA: Prentice-Hall.
- Sohl, G. A. and Bobrow, J. E.** 1997. Experiments and Simulations on the Nonlinear Control of a Hydraulic Servosystem. *Proceedings of American Control Conference*, Albuquerque, Novo Mexico.
- Virtanen, A.** 1993. The design of state controller of hydraulic position servo system. *3rd Scandinavian International Conference on Fluid Power*, Linköping, pp. 193-206.
- Virvalo, T.** 1997. Nonlinear Model of Analog Valve. *5th Scandinavian International Conference on Fluid Power*, Linköping, Vol. 3, pp. 199-213.
- Yao, B., Bu, F., Reedy, J. T. and Chiu, G. T. C.** 2000. Adaptive Robust Motion Control of Single-Rod Hydraulic Actuators: Theory and Experiments. *Transactions on Mechatronics*, Vol. 5, No. 1, pp. 79-91.



Mauro André Barbosa Cunha

Born on March 30th 1972 in Pelotas-RS (Brazil). Study of Electrical Engineering at UCPEL Pelotas-RS. Doctor in Electrical Engineering at UFSC in April 2001. At the moment, he is an assistant professor at Pelotas Federal Centre for Technological Education.



Raul Guenther

Born on May 27th 1953 in Joinville (Brazil). Study of Mechanical Engineering at UFSC Florianópolis-SC. Doctor in Mechanical Engineering at UFRJ in 1993. He is professor in Mechanical Engineering Department at UFSC. At the moment, he is the head of the Robotics Laboratory.



Edson Roberto De Pieri

Born on May 30th 1960 in Mogi Mirim (Brazil). Study of Mathematics at UNICAMP Campinas-SP. Doctor in 1991 at Université de Paris VI in Electrical Engineering. He is professor in Automation and System Department at UFSC. At the moment, he is the head of the Electrical Engineering Post Graduation Program.



Victor Juliano De Negri

Born on September 15th 1960 (Brazil). Study of Mechanical Engineering at UNISINOS São Leopoldo-RS. Doctor in Mechanical Engineering at UFSC in 1996. He is professor in Mechanical Engineering Department at UFSC. At the moment, he is the head of the Laboratory of Hydraulic and Pneumatic Systems.